

# Source Space Minimization Technique for MEG Source Analysis

J.E. Moran<sup>1</sup>, and N. Tepley<sup>1,2</sup>.

<sup>1</sup>Henry Ford Hospital, Detroit, Michigan USA; <sup>2</sup>Oakland University, Rochester Michigan USA  
(tepley@oakland.edu)

## Introduction

The magnetic inverse solution of:

$$\mathbf{b} = \mathbf{G}\mathbf{q},$$

can be transformed into a minimization of:

$$[\mathbf{b} - \mathbf{G}\mathbf{q}]^2$$

with a least squares solution:

$$\mathbf{q} = [\mathbf{G}^T\mathbf{G}]^{-1}\mathbf{G}^T\mathbf{b}$$

$\mathbf{b}$  = vector of M data channels

$\mathbf{q}$  = vector of N source parameters

$\mathbf{G}$  = matrix of parameter magnetic fields  
with (M > N)

Alternatively, the equation can be solved by refining an initial solution estimate  $\mathbf{q}_0$ , by a gradient descent method [1]:

$$\mathbf{q}_{i+1} = \mathbf{q}_i + \alpha_i[\mathbf{G}^T\mathbf{G}]^{-1}\mathbf{G}^T\mathbf{r}_i \quad (1)$$

$$\mathbf{r}_{i+1} = \mathbf{r}_i - \mathbf{G}(\mathbf{q}_{i+1} - \mathbf{q}_i)$$

The gradient decent technique is commonly used to determine an equivalent current dipole solution where the source vector incorporates both amplitude and location:

$$\mathbf{q} = [q_x \ q_y \ q_z \ x_q \ y_q \ z_q]$$

However, for both source solutions, the components of  $\mathbf{b}$  corresponding to low amplitude eigenvalues in spectrum of the matrix  $[\mathbf{G}^T\mathbf{G}]$  are amplified. This is undesirable, especially if  $\mathbf{b}$  contains noise. As an alternative to regularization techniques, the excessive sensitivity to small eigenvalue components of  $\mathbf{b}$  can be avoided by performing a source space minimization of:

$$[\mathbf{G}^T\mathbf{b} - \mathbf{G}^T\mathbf{G}\mathbf{q}]^2 \quad (2)$$

with the recursive solution:

$$\mathbf{q}_{i+1} = \mathbf{q}_i + \alpha_i[\mathbf{G}^T\mathbf{G}]\mathbf{G}^T\mathbf{r}_i \quad (3)$$

$$\mathbf{r}_{i+1} = \mathbf{r}_i - \mathbf{G}(\mathbf{q}_{i+1} - \mathbf{q}_i)$$

$$\alpha_i = \mathbf{r}_i^T[\mathbf{G}\mathbf{G}^T]^2\mathbf{r}_i / \mathbf{r}_i^T[\mathbf{G}\mathbf{G}^T]^4\mathbf{r}_i.$$

This recursive solution amplifies the importance of large eigenvalue components of the magnetic field rather than the small ones. A sufficiently accurate solution is obtained when the number of iterative steps is equal to the rank of the matrix,  $\mathbf{G}^T\mathbf{G}$ , (Eqn. 1). Thus, it is an efficient technique if the matrix,  $\mathbf{G}^T\mathbf{G}$ , is small. The rank

of  $\mathbf{G}^T\mathbf{G}$  is two at each cortical location if  $\mathbf{G}$  is based on a spherical head model and rank 3 if the forward solution incorporates a realistic head model such that radial sources generate detectable magnetic fields. In addition, Equation 3 is utilized in our 2DII imaging technique where the rank of  $\mathbf{G}^T_{2DII}\mathbf{G}_{2DII}$  is four [2, 3].

## Methods

The accuracy of this minimization technique was tested by using Equation 2 to calculate  $[q_x \ q_y \ q_z]$  at 16 locations on a 0.6 cm square grid, within a MEG sensor array. In Figure 1, a spherical volume conductor forward model of the head was used to generate 148 channels of magnetic field data corresponding to a current dipole oriented successively in the x, y, or z direction at one grid location. The z orientation is almost radial relative to the chosen sphere origin. For these three sets of simulated data, Equation 3 was used to solve for the solution vector,  $\mathbf{q}$ , at each grid position. In addition, for each of the 16 grid points, the fractional magnetic field power mismatch of the source solution was calculated:

$$\text{ERROR} = |\mathbf{b} - \mathbf{b}_{\text{grid\_pt}}|^2 / |\mathbf{b}|^2.$$

and

$$\text{goodness of fit} = 1 - \text{ERROR}.$$

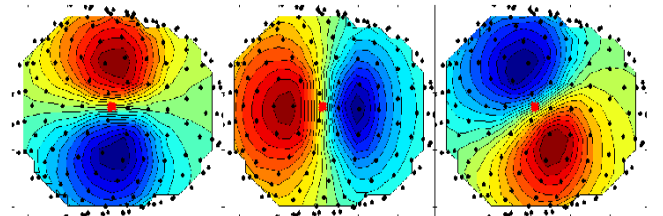


Figure 1: left to right, Magnetic field of x, y, and z oriented dipole within a small patch of 16 source imaging locations, (red patch). Black dots are at 148 MEG detector locations, (top view).

Finally, imaging software incorporating this technique was applied to patient data to generate equivalent current dipole (ECD) and 2DII [1] images of visual evoked cortical activity.

## Results

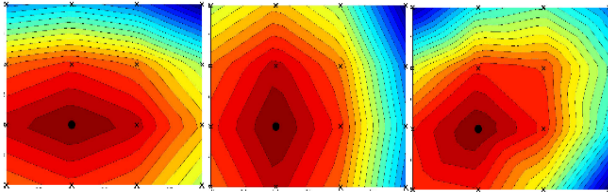


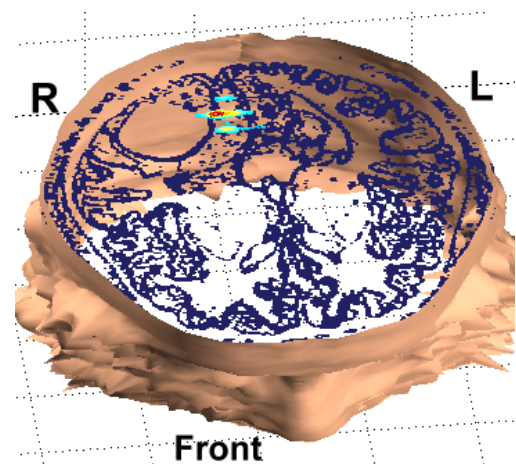
Figure 2: Goodness of fit contour plots for source solutions at 16 grid locations, (black x), Active current dipole at black dot with current dipole orientation in the x (left), y (center), z (right) direction. The Magnetic fields of these sources are in Figure 1. The goodness of fit of the solution was 100 percent at the grid location corresponding to the active source.

	x amp	y amp	z amp
x oriented dipole	0.9994	-0.0006	-0.0250
y oriented dipole	-0.0006	0.9994	-0.0250
z oriented dipole	-0.0250	-0.0250	0.0012
radial direction vector	0.0250	0.0250	0.9994

Table 1: The orientation of a unit amplitude simulated current dipole source is in first column. The x, y, and z amplitudes of the corresponding source solution at the active grid site are in columns 2-4. The x, y, and z components of the radial direction vector of the sphere model at this site is included to demonstrate that the source solutions are purely tangential. Thus, only the small tangential component of the z oriented source is magnetically visible.

In Figure 2, the goodness of fit for the solution, (Equation 3), is 1.0 at the true source location. At each of 16 grid locations, the source solutions,  $\mathbf{q}$ , (Equation 3), were tangential to the spherical volume conductor model used to generate the simulated data and forward solutions. These results are tabulated in Table 1 for the grid location corresponding to the simulated source. The goodness of fit for 16 source solutions within the 0.6 cm square grid ranged from 98.2 to 100 percent at the actual source location, Figure 2. For these spherical head model results, only 2 iterative steps were required to calculate each ECD solution,  $\mathbf{q}$ . Three iterative steps would be required if the forward solution incorporated a realistic model of the patient's head geometry.

Figure 3 depicts the results of applying Equation 3 to visual evoked field data of a patient with a right occipital tumor. The latency was 167 milliseconds after checkerboard pattern reversal within the left visual field. The three dimensional view is derived from the patient MRI data. Using the MRI data, the cortical gray mater was modeled with a three dimensional grid of 2955 grid points and Equation 3 applied at each point to determine  $\mathbf{q}$  and the corresponding goodness of fit. At the center of the red false color area, the goodness of fit was 98.1 percent and the localization error



estimated to be less than two millimeters.

Figure 3: Equivalent current dipole goodness of fit metric generated with Equation 3 for left visual field data. The adjacent outline of the Occipital tumor is visible.

The 2DII whole brain source activation image for this patient data is an average of 32 2DII source amplitudes for the time window 167 to 228 milliseconds after pattern reversal, Figure 4. The 2DII technique converts the underdetermined continuum model of the cortex to an iterative solution of a sequence of overdetermined source solutions where the rank of  $\mathbf{G}^T_{2DII} \mathbf{G}_{2DII}$  is four.

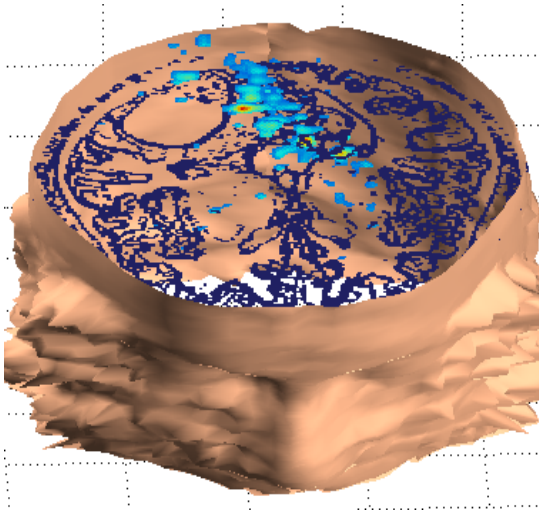


Figure 4: The average of 32 2DII source solutions for 167 to 228 milliseconds after checkerboard pattern reversal within the left visual field.

## Discussion

The iterative solution of Equation 2 is a conjugate direction minimization technique [4]; the sequence of residual magnetic field vector changes are orthogonal,  $\Delta \mathbf{r}_i \Delta \mathbf{r}_j = 0$ . Although the algorithm operates on the residual field,  $\mathbf{r}_i$ , the final solution can be represented as:

$$\mathbf{q} = \sum \beta_i [\mathbf{G}^T \mathbf{G}]^{2i-2} \mathbf{G}^T \mathbf{b}, i \geq 2.$$

This form of the solution can also be obtained by using the characteristic equation of the matrix  $[\mathbf{G}^T \mathbf{G}]$  to construct a series expansion for  $[\mathbf{G}^T \mathbf{G}]^{-1}$  in powers of  $[\mathbf{G}^T \mathbf{G}]$ .

For these single current dipole results, the set of equations required for the series expansion is:

$$\begin{aligned} [\mathbf{G}^T \mathbf{G}]^{-1} \{ \beta_3 [\mathbf{G}^T \mathbf{G}]^3 + \beta_2 [\mathbf{G}^T \mathbf{G}]^2 + \beta_1 [\mathbf{G}^T \mathbf{G}] + \beta_0 \} &= 0 \\ \dots \{ \dots + \dots + \dots + \dots \} &= 0 \\ [\mathbf{G}^T \mathbf{G}]^6 \{ \beta_3 [\mathbf{G}^T \mathbf{G}]^3 + \beta_2 [\mathbf{G}^T \mathbf{G}]^2 + \beta_1 [\mathbf{G}^T \mathbf{G}] + \beta_0 \} &= 0 \end{aligned}$$

$\beta_k$  are characteristic equation coefficients.

However, the iterative construction of the solution using Equation 3 is efficient and easy to adapt to matrices of different rank. In addition when applied to real MEG data the number of terms in the solution can be truncated when the residual field is primarily noise. The application of this technique to calculate 2DII source solutions and equivalent current dipole source amplitudes demonstrates the efficiency of this technique when the matrix,  $[\mathbf{G}^T \mathbf{G}]$ , is small

**Acknowledgement:** Research supported by NIH/NINDS Grant RO1-NS30914.

## References

1. M. Hämäläinen, R. Hari, R.J. Ilmoniemi, J. Knuutila and O.V. Lounasmaa Magnetoencephalography theory, instrumentation, and applications to noninvasive studies of the working human brain Rev. Mod. Phys., 1993, 65: No. 2 413-495
2. J.E. Moran, N. Tepley, Two Dimensional Inverse Imaging (2DII) of Current Sources in Magnetoencephalography, *Brain Topography*. 12 no. 3, 2000, 201-217.
3. J.E. Moran, N. Tepley, Two Dimensional Inverse Imaging (2DII) applied to large array magnetoencephalographic data, in Recent Advances in Biomagnetism, T Yoshimoto et. al. Eds. , Tohoku University Press, Sendai, 1999, 270-273
4. WH Press, *Numerical Recipes in C*, 2ed., (Cambridge University Press New York, 1996), 413-416.